Received: 12 June 2022 | Revised: 15 August 2022 | Accepted: 8 September 2022

DOI: 10.1002/er.8765

RESEARCH ARTICLE

INTERNATIONAL JOURNAL OF ENERGY RESEARCH WILEY

Testing of the oil-immersed sensible heat storage unit with circular channel solid heat body under charging modes with different heat transfer temperature difference

Fangzheng Cheng[1] | **Yang Zou**[2] | **Shengyao Huang**[1] | **Xinyi Wang**[2] | **Xinfeng Yu**[1] | **Weiwei Ma**[1] | **Hao Zhou**[1]

[1]State Key Laboratory of Clean Energy Utilization, Institute for Thermal Power Engineering, Zhejiang University, Hangzhou, China

[2]Shanghai Boiler Works Co., Ltd, Shanghai, China

Correspondence
State Key Laboratory of Clean Energy Utilization, Institute for Thermal Power Engineering, Zhejiang University, Hangzhou 310027, China.
Email: zhouhao@zju.edu.cn

Funding information
National Natural Science Foundation of China, Grant/Award Number: 52036008

Summary

Heat storage technology can enrich and store dispersed and discontinuous heat and significantly improve energy efficiency. This paper reports a pilot-scale sensible heat storage unit, which uses circular channel solid made of castables as the heat storage bodies and heat transfer oil as the working fluid. When performing, the heat transfer oil passes through the flow channel of the heat storage body and is in direct contact with the heat storage body for heat exchange. The experiment explores the unit's thermal performance, including heat, power, and charge energy efficiency under different charging temperature difference modes. At the same time, the normalized charge energy efficiency is used to evaluate the heat-storage unit's heat absorption capacity during the charging process. The results show that the average heat storage capacity of the heat storage body is about 1.10×10^6 kJ, accounting for 89% of the heat storage capacity of the unit, and the remaining 11% is the heat stored in the oil inside the unit. In addition, the charging mode with step temperature rise used in the experiment can make the heat stored by the regenerator increase linearly with time. The charging mode with a more considerable temperature difference can significantly enhance the charging power and shorten the charging time, but the increase in the temperature difference reduces the efficiency of the charging process. The efficiency in the experimental range is reduced from 64.5% in the minimum temperature difference mode to 34.8% in the maximum temperature difference mode. This paper has a certain supplementary function for the design and application of heat storage and the evaluation of the thermal performance of the heat storage unit.

KEYWORDS

charge energy efficiency, circular channel solid heat storage body, contact heat transfer directly, heat transfer oil, sensible heat storage unit

1 | INTRODUCTION

Using energy is the driving force of production and life in human society. From the use of biomass energy, which has the most extended history, to the fossil energy that promoted the human industrial revolution, to the clean and renewable energy that is vigorously advocated around the world today, such as solar energy, geothermal

energy, and wind energy, our energy structure is constantly being adjusted and optimized.[1] As the concept of sustainable development is deeply rooted in the people's hearts and a human community with a shared future has gradually become a consensus, many countries have made carbon emission reduction a priority in the first 60 years of this century worldwide, turning to non-polluting and renewable energy and vigorously developing renewable resources, including solar energy.[2,3] For renewable energy today, such as wind and solar energy, its shortcomings, such as intermittent and uneven distribution, restrict human beings' direct and rational utilization. In addition, the mismatch between supply and demand in the energy system further limits human beings' effective utilization of energy.[4,5] To take full advantage of renewable energy, heat storage technology has received attention from energy practitioners, which provides an excellent opportunity for the development of energy storage rapidly. Sensible heat storage, latent heat storage and thermochemical heat storage technology are essential in different application scenarios.[6]

The sensible heat storage technology has strong adaptability in different scenarios, so it has been rapidly developed and applied. Various materials are used for sensible heat storage, including molten salt, heat transfer oil (HTO), and solid materials. Among them, solid heat storage materials have received extensive attention and research. Common solid heat storage materials, including sand, rock, and metal particles, are distributed worldwide and are easy to obtain and use.[7]

In the previous research, the solid material was commonly used to be the medium in the heat storage technology, where the particles are randomly stacked in the stacked bed, and the working fluid flows through the particle gap while exchanging heat with the solid. A. Wake and Pitam Chandra et al[8,9] studied the energy storage performance of rocks with different particle sizes under different air flow rates. In the experiment, 80% to 90% of the stored energy was recovered, and the heat transfer coefficient and pressure drop mainly depend on the particle's diameter and flow rate of the working fluid; the research content provides a feasible reference for solar thermal storage. M.M. Sorour et al[10] investigated the heat storage performance of the gypsum rock particle packed-bed and revealed that the principal factors such as the size of the heat storage unit and the particle's diameter affect the energy storage efficiency. M.A. Keilany et al[11] conducted heat charging and exothermic experiments when Cofalit and alumina pellets were used as heat storage fillers, respectively, and found that Cofalit had a better thermal performance. Rohan Dutta et al[12] established a thermal storage experimental device by filling the bed with pebble material and determined the device's storage efficiency under full-load and partial-load operations.

In the fixed bed method, multi-channel solid heat storage is mainly used for sensible heat storage. Stefano Soprani et al[13] tested the thermal performance of rock beds as a heat storage unit, including thermal charging power, rock bed layout, and efficiency. Valentina A. et al[14] studied the application of concrete regenerators in solar thermal power plants and carried out related optimizations. K. Vigneshwaran et al[15] designed and prepared a heat storage unit with metal tubes embedded in the concrete body, laying the foundation for the practical application of concrete in industry. Using air as the working medium, Ravi Kumar et al[16-18] investigated the heat storage performance of multi-channel concrete regenerators and found that inserts in the flow channel can significantly improve the operating efficiency.

Many researchers use energy efficiency and exergy efficiency to evaluate the performance of a heat storage unit or heat storage system to measure heat utilization in itself. Hitesh Bindra et al[19] developed a heat transfer model for the packed-bed system and calculated the recovered and lost exergy to evaluate the heat recovery capability of the system effectively. Al-Azawi et al[20] studied the alumina-packed bed experimentally and used the exergy index to evaluate the heat storage system under different fluid flow rate conditions. Öztürk et al[21] conducted energy efficiency and exergy efficiency analysis on an underground thermal energy storage system and explored the influence of the temperature of the heat exchange fluid and the surrounding environment on the thermal energy storage system.

However, solid heat storage is mainly in the form of a stacked bed heat storage, and the thermal energy storage method using a fixed bed is often accompanied by a metal tube embedded in a solid heat storage body (HSB). The former undoubtedly causes uneven flow velocity distribution in different areas inside the heat accumulator, and the latter increases the heat exchange end difference (HEED)due to embedding the metal tube in the solid HSB. The HEED causes a gap between the tube and the HSB, and the body is affected by thermal stress to produce cracks,[22] increasing the heat transfer resistance and deteriorating the heat transfer effect. In addition, many studies mostly explore the effect of different flow rates of the working fluid on the thermal performance; the research on the effects of different charging temperature differences on the operating performance of the heat storage unit is still not sufficient. Therefore, this paper attempts to study a sensible heat storage unit (SHSU) with the circular channel solid heat storage body immersed in HTO to avoid the problem of increased thermal resistance caused by the generation of gaps and

cracks and to explore the influence of different modes of heat transfer temperature difference on the performance of the unit. The unit's thermal performance under different heat transfer temperature difference charging modes is experimentally studied, and oil and solid's respective heat and power changes during the charging process are analyzed. The efficiency of the charging model was evaluated. This unit with the circular channel solid HSB immersed by HTO, not by air with a smaller specific heat capacity in this study, which is an attempt at sensible thermal energy storage and provides new ideas for heat recovery and storage in the process of production and life, as well as the design and application of heat storage device.

2 | EXPERIMENTAL SETUP AND CASE

Figure 1 is a diagram of the experimental system. The experimental system includes an HTF circulation heater with a total output rated power of 225 kW (as is shown in Figure 2), which can heat the HTF to the temperature required for our experiments, a sensible heat storage device, a cooling device, data acquisition equipment, auxiliary pipelines and valves. The working fluid is heated to the set temperature during the charging experiment, starts from the HTF circulation heater, enters the SHSU, flows evenly into the flow channel of the HSB after passing through the flow uniform distributor, and directly contacts with the HSB for heat transfer. After heat exchange between HSB and working fluid, the working fluid flows out of the SHSU and returns to the HTF circulating heater. The cooling device in the experimental system is used to cool the working fluid during the discharging.

The SHSU with a cylindrical shape is the heat storage device in the experimental system; as shown in Figure 3, the tank material of SHSU is Q235; its size is 1320 mm × 4500 mm (diameter × height) and contains three identical multi-channel cylindrical HSBs. Figure 4 is the schematic diagram of the HSB, the parameters of

FIGURE 2 The photo of the working fluid circulation heater

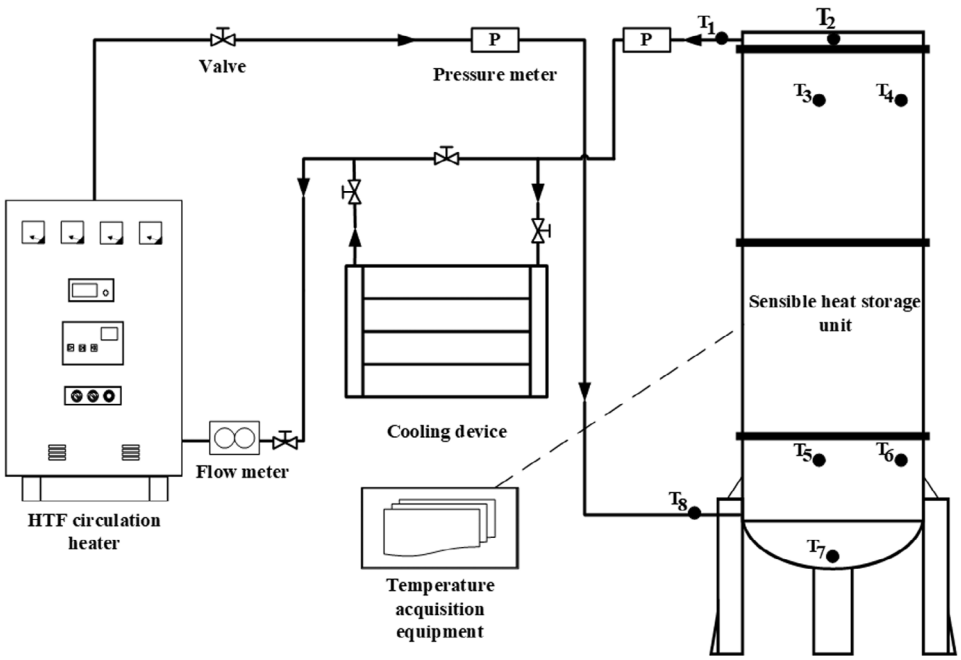

FIGURE 1 The diagram of the experiment system ($T_{\#}$ are the thermocouples)

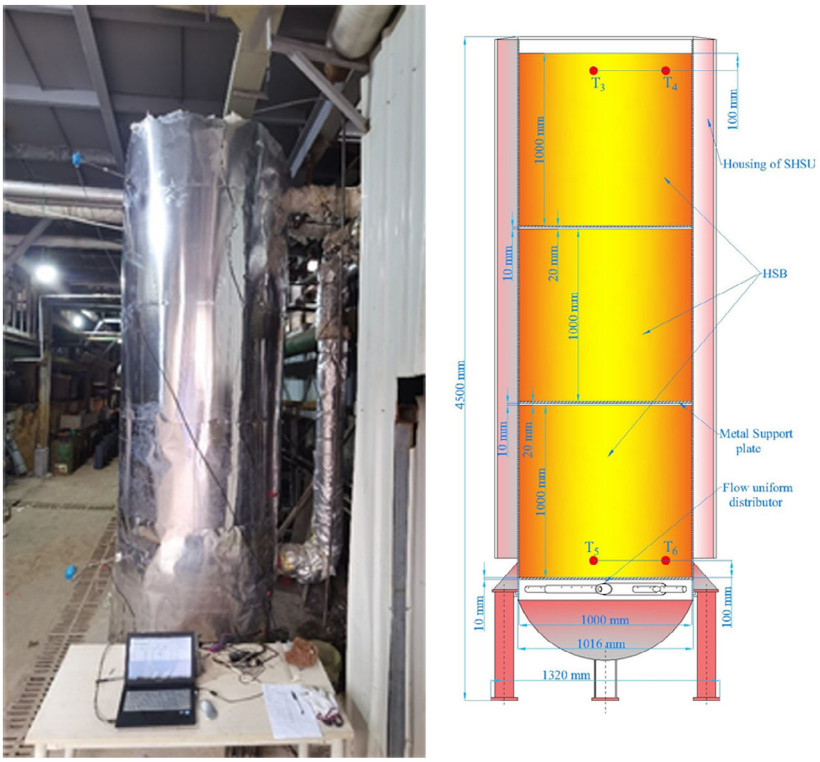

FIGURE 3 The SHSU used in the experiment (left) and the schematic of its overall structure (right) ($T_{\#}$ are the temperature measurement points)

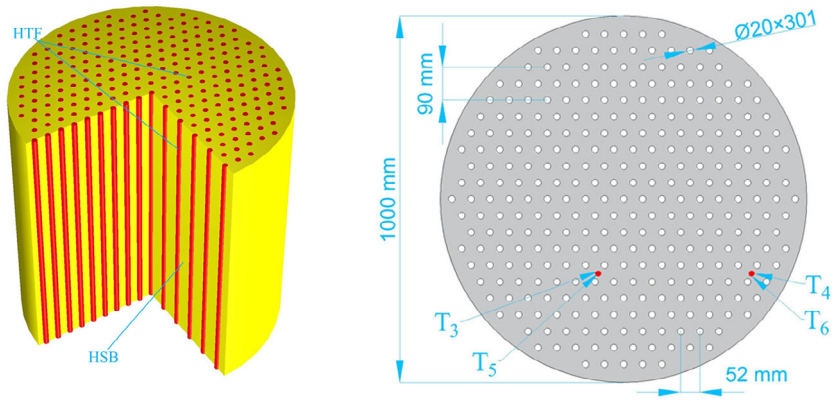

FIGURE 4 The diagram of HSB dissection (left) and its radial cross-section diagram (right) ($T_{\#}$ are the temperature measurement points)

TABLE 1 Thermal properties of HSB and HTO

Material	Density (kg/m^3)	Specific heat capacity (MJ/m^3 K)	Thermal conductivity (W/m K)
HSB	2797	2.42	3.97
HTO	1011	1.294	0.1225

the HSB are 1000 mm × 1000 mm(diameter × height), using common corundum castables as heat storage material (thermal properties of material measured in the laboratory are shown in Table 1. In order to make the fluid flow through the HSB more evenly and carry out effective heat transfer, the HSB is constructed with 301 cylindrical fluid channels of the same size, and the diameter of each channel is 20 mm. With a flow uniform distributor arranged at the bottom, the location of the flow uniform distributor is shown in Figure 3. As shown in Figure 5, the flow uniform distributor is an axisymmetric component, the trunk is the axis of symmetry, and all branches are centrally symmetrical. When the system is working, the working fluid first enters the trunk of the flow uniform distributor and then flows out of the through-holes on the branches of the flow uniform distributor, so the HTF entering the heat storage device can flow into each fluid channel of the HSB evenly. The working fluid

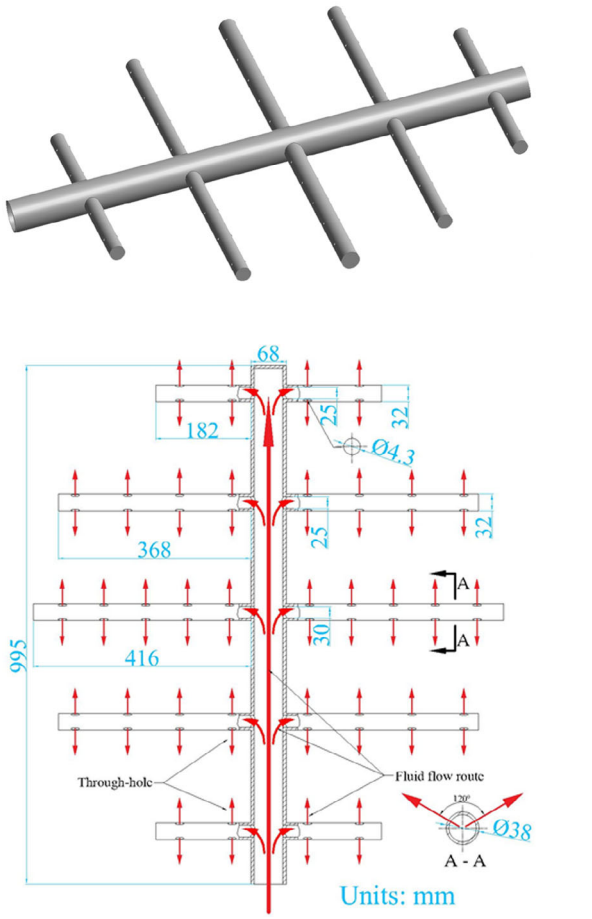

FIGURE 5 Model of flow uniform distributor (up) and Schematic diagram of fluid flow route inside the flow uniform distributor (down)

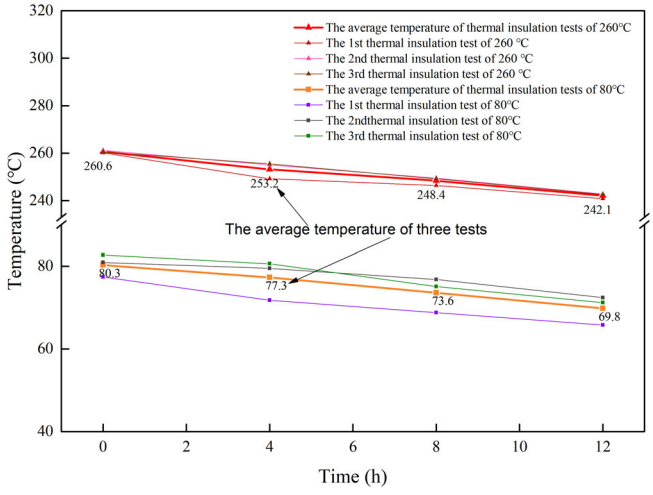

FIGURE 6 Average HSB temperature change during insulation testing

adopts Therminol L-60 synthetic heat transfer oil, a highly efficient and stable working fluid that can transfer heat usually between −17 and 320°C. The outer wall of SHSU is wrapped with thermal insulation cotton, which can effectively reduce the heat loss of SHSU. The thermal insulation test results are shown in Figure 6.

During the actual test, the k-type thermocouple measures the temperature with an accuracy of 0.5°C. An Agilent 34970A data acquisition device records temperature data, and a computer is used to collect the data. A LUGB-1204 vortex flowmeter obtained the flow measurement data with an accuracy of 1%. Before the formal experiment, the temperature and flow rate devices were calibrated.

In this study, charging experiments with different temperature gradients were carried out using different temperature difference modes; that is, the temperature difference between the inlet working fluid and the HSB was maintained within a specific range during the charge. For all the charging experiments, the temperature of the HSB at the beginning of the charging is 80°C, and the working fluid's temperature is 140°C; at the end of the charging, the working fluid's temperature is 290°C, and the corresponding average HSB's temperature is 260°C, the minimum temperature difference during the entire charging process is 30°C. The mass flow rate of the working fluid is 2.0 kg/s. The difference between each working condition of different step temperature rises is that the gradient of the temperature rise at the outlet of the working fluid circulating heater (it is also the SHSU's inlet temperature) is different. According to this difference, the test conditions are named Case-10, Case-20, Case-30, Case-40, and Case-50, and the different experimental cases are shown in Table 2.

The difference in each experimental case is that when the difference between the SHSU's inlet temperature (T_8) and the HSB's temperature (the reference point is selected as T_3) drops to 30°C, the inlet temperature increment of SHSU is different. For example, for Case-10, when the difference between the SHSU's inlet temperature and the HSB's temperature drops to 30°C, the SHSU's inlet temperature is increased by 10°C accordingly, until the final temperature was 290°C.

3 | DATA ANALYSES

When the thermal energy storage system works, the HTF releases or absorbs the heat in the heat storage unit. Therefore, the temperature difference of the HTF at the inlet and outlet of the solid heat storage can be considered to obtain the cumulative energy input or absorbed by the HTF in the heat storage unit, as shown in Equation (1).

TABLE 2 The experimental case

Experimental case	The increment of SHSU's inlet temperature (°C)	The initial SHSU's inlet temperature (°C)	The final SHSU's inlet temperature (°C)	The range of HSB's temperature (°C)
Case-10	10	140	290	80 ~ 260
Case-20	20	140	290	80 ~ 260
Case-30	30	140	290	80 ~ 260
Case-40	40	140	290	80 ~ 260
Case-50	50	140	290	80 ~ 260

$$E = \int_0^t q_m c_p (T_{\text{in}} - T_{\text{out}}) dt = \int_0^t \rho q_v c_p (T_{\text{in}} - T_{\text{out}}) dt \quad (1)$$

where ρ is the density of HTF, q_v is the volume flow rate, c_p is the specific heat capacity of HTO, and T_{in} and T_{out} are the unit's inlet and outlet oil temperature respectively.

The experimental HTO density is calculated by Equation (2).

$$\rho(T) = -0.81447T + 1029.05546 \quad (2)$$

The specific heat of the HTO at different temperatures is calculated by Equation (3).

$$c_p(T) = 0.00461T + 1.17333 \quad (3)$$

Average power is the average of the total energy throughout the process, as shown in the following Equation (4).

$$P = \frac{\int_0^t q_m c_p (T_{\text{in}} - T_{\text{out}}) dt}{t} \quad (4)$$

The internal cavity of the heat accumulator is about 0.5 m^3. Partial energy is stored and released by the HTO, which exists in the cavity inside the SHSU, and is heated and cooled while the charging and discharging. This heat is defined as the heat stored in the oil, calculated as follows.

$$Q_{\text{oil}} = \int_{T_1}^{T_2} \rho_e V_{\text{oil}} c_p(T) dT \quad (5)$$

In Equation (5), ρ_e is the density of the HTO at the end of the charge; $c_p(T)$ is the specific heat capacity of the HTO during the charge, calculated according to the qualitative temperature of the process; T_1 and T_2 are the temperature of the HTO at the end of the charge and discharge, respectively; V_{oil} is the volume of HTO equal to the cavity volume inside the unit.

The heat dissipation loss of the unit under the experimental conditions is calculated to analyze the heat accumulator's capacity more accurately by Equation (6).

$$Q_{\text{lose}} = c_{\text{p.solid}} V_{\text{solid}} \dot{T} t_n \quad (6)$$

where $c_{\text{p.solid}}$ is the specific heat capacity of the HSB; V_{solid} is the volume of the solid regenerator; t_n is the time used for the charge and discharge; $\dot{T}$ is the rate of temperature drop under experimental conditions, equal to 1.2°C/h, which is obtained from the thermal insulation testing, the results of thermal insulation testing are shown in Figure 6;

The heat in the heat storage experimental system consists of the heat in the HSB, the heat stored in HTF in the cavity inside the SHSU, and the SHSU's heat dissipation to the environment. Therefore, the heat stored by the regenerator in the HSB can be calculated from the heat balance during charge.

$$Q_{\text{cha.storage}} = E - Q_{\text{cha.oil}} - Q_{\text{cha.lose}} \quad (7)$$

Charge energy efficiency is determined by the amount of energy stored by a sensible thermal storage system at a particular moment and the amount of energy supplied. It represents the ability of the storage system to absorb thermal energy.[23]

$$\eta_e = \frac{T_{\text{ave}} - T_i}{T_{\text{in}} - T_i} \quad (8)$$

where T_{in} is the inlet temperature of the unit; T_i is the initial temperature of the HSB; T_{ave} is the average temperature of the HSB calculated by Equation (9).

$$T_{\text{ave}} = \frac{T_3 + T_4 + T_5 + T_6}{4} \quad (9)$$

Since the time spent in the charge varies depending on the charging mode used, to more intuitively measure the thermal energy absorption capacity of the thermal energy storage system in the entire charging process

under different modes, we define a normalized charge energy efficiency. The parameter of charging time is introduced to effectively evaluate the relative size of the SHSU's energy efficiency during the charging process.

$$\eta_n = \frac{\int_0^{t_x} \eta_e(t)dt}{t_{\max}} \tag{10}$$

where t_x is the time spent in a particular charging experiment, $t_{\max}$ is the charging time corresponding to the working condition that takes the longest time among all the experimental charging conditions, and t is the charging experiment time.

In the study, the method reported by Moffat[24] is used to estimate the uncertainties of the dependent parameters. The Equation (11) gives the uncertainties due to the individual uncertainties of the independent parameters.

$$\Delta Y = \sqrt{\left[\frac{\partial Y}{\partial z_1}\Delta z_1\right]^2 + \left[\frac{\partial Y}{\partial z_2}\Delta z_2\right]^2 + \left[\frac{\partial Y}{\partial z_3}\Delta z_3\right]^2 + \ldots + \left[\frac{\partial Y}{\partial z_n}\Delta z_n\right]^2} \tag{11}$$

where ΔY is the uncertainty of the performance parameter and Δz_1, Δz_2, Δz_3, ... Δz_n are the errors in dependent variables in the evaluation of z_1, z_2, z_3, ... z_n.

4 | RESULTS AND DISCUSSION

4.1 | The temperature of different case

Figure 7 shows the changes in the temperature of the HTO at the SHSU's inlet as well as outlet and the average temperature of the internal HSB during the entire charging process under different charging conditions. Under the experimental setting conditions, the inlet HTO's temperature increased from 140°C to 290°C according to different stepped temperature rise modes. Obviously, the HSB's temperature change increases linearly during the whole heat charging process, while the temperature of the outlet HTO fluctuates significantly due to the change in the inlet HTO's temperature. The reason can be that the HTO with a higher temperature entering the heat storage unit transfers heat to the HSB through convection heat exchange. However, the oil with a lower temperature inside the heat storage unit is mixed with the newly entered working fluid with a higher temperature. The latter transfers heat with higher thermal efficiency, showing noticeable temperature disturbance more quickly.

4.2 | Charging time

The variation of the HSB's temperature under the charging process experimental conditions is shown in Figure 8. The HSB's temperature increases linearly with time during the whole thermal charging process under different thermal charging experimental conditions, which is related to the fact that the working medium and the thermal storage medium maintain a specific temperature difference during the thermal charging process. Case-10 showed the best linear relationship in all working conditions (The linearity of Case-10, $R^2 = 0.9993$, is the largest in all experimental conditions), which mainly depended on the temperature difference between the HTF and the HSB was kept small during the whole heat charging process in this working condition. According to the current experimental results, we can see that increasing the temperature difference between the working fluid and the HSB during the heat charging process makes the temperature change curve of the HSB steeper; that is, increasing the heat transfer temperature difference can increase the heat transfer rate and shorten the heating time. When using the charging method under the temperature difference mode corresponding to Case-10, the time consumed is 250.1 minutes; when the temperature difference increases to the Case-50 mode, the time it takes for the HSB to be heated to the same temperature is only 159.9 minutes, down 36.1%. From another point of view, we know that the case with a large heat transfer temperature difference during the charging process can obtain a higher temperature of the HSB in the same amount of time. In other words, if we want to obtain enough heat in a short time, we can choose the large temperature difference charging mode for heat charging in practical applications.

4.3 | The outlet temperature

Figure 9 shows the change curve of the HTO's temperature at the outlet of the heat storage unit with time during the charging process under different conditions. The temperature of HTO at SHSU's outlet at the end of charging will not be significantly different due to different temperature difference charging modes, and the outlet HTO's temperature is about 272°C. Due to the different charging modes, the temperature growth speed of the HTO at the outlet of the SHSU is different during the whole charging process. For the case with a more considerable temperature difference, the fluctuation trend of the temperature curve is more prominent, and the temperature growth rate changes significantly.

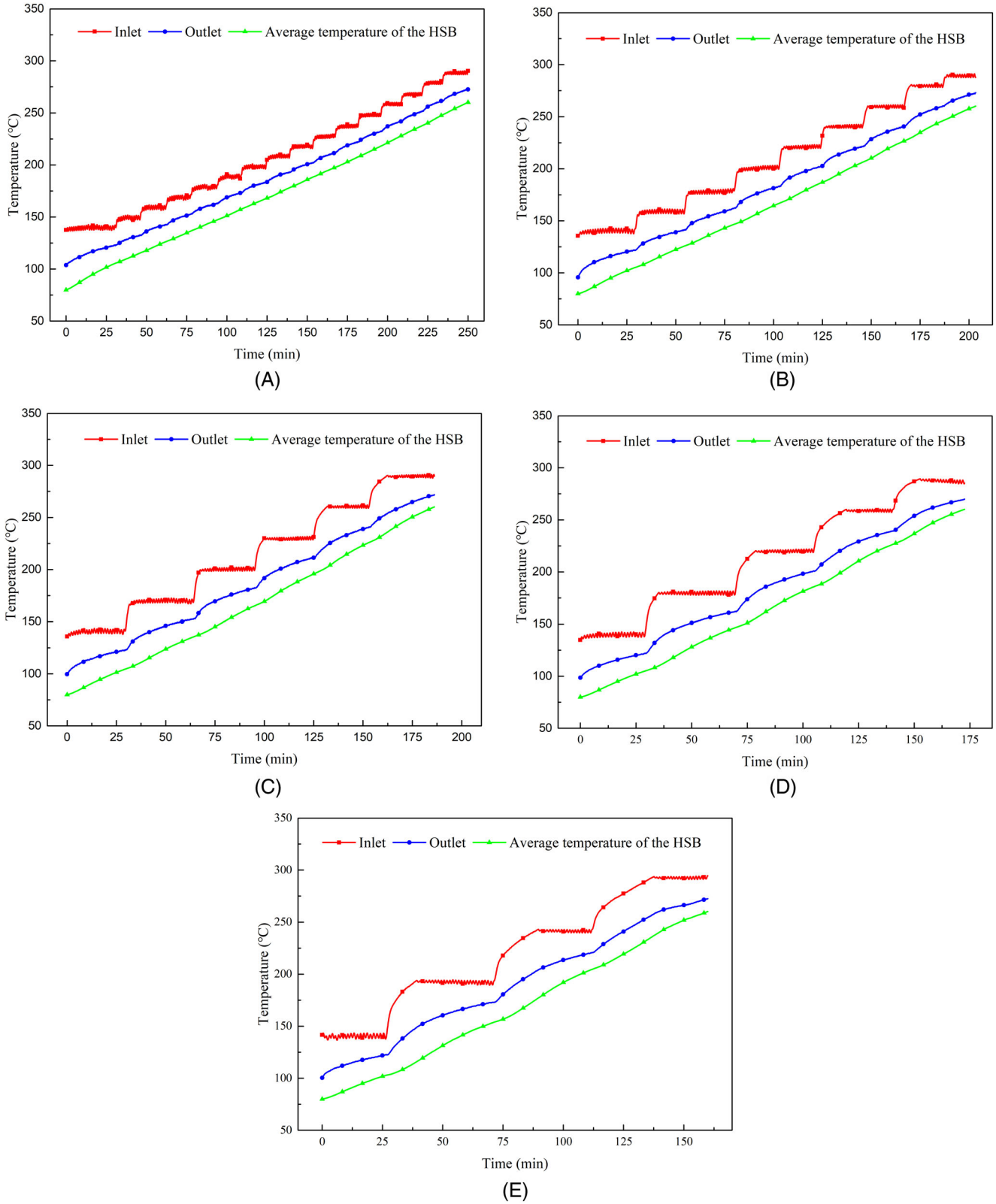

FIGURE 7 Temperature change of heat storage unit under different charging modes

In contrast, the temperature difference in the minor charging mode, the temperature increase rate is relatively stable. In the case with a large temperature difference, the temperature rise curve is steeper, which means that the heat transfer rate is faster in the charging process.

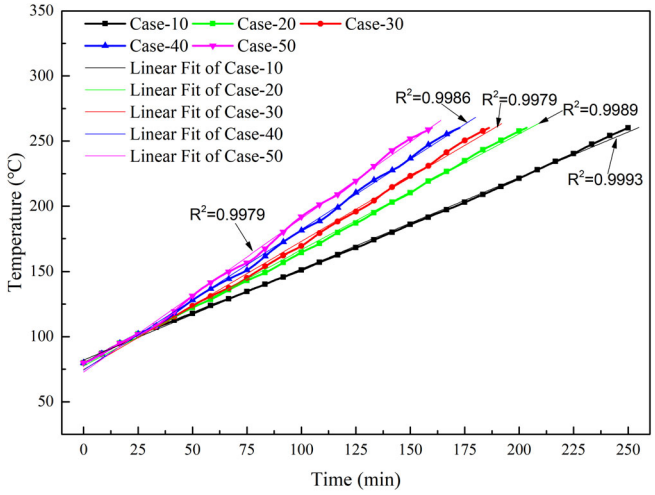

FIGURE 8 The average temperature of the HSB changes with time

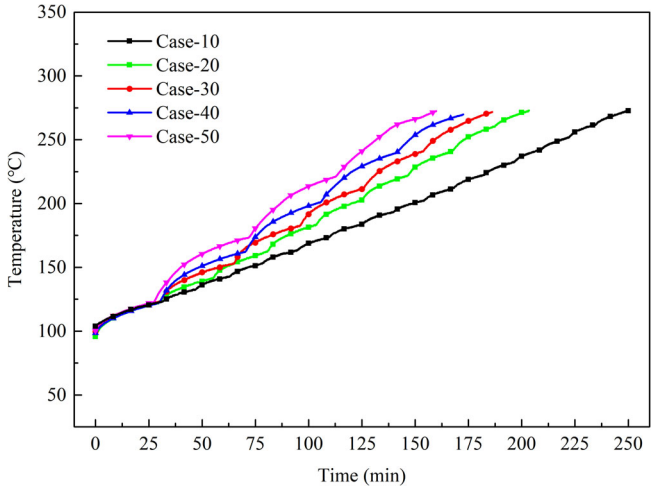

FIGURE 9 The temperature change of the HTO at the outlet of the heat storage unit

4.4 | Energy classification

To more intuitively compare the heat change in the SHSU under different charging modes, We divide energy into three categories, including the heat released by the HTO (HTO input energy), the heat stored in the HSB (HSB stored energy) and the heat stored in the HTO itself (HTO stored energy) in the unit during the heat charging process. Figure 10A, B shows the evolution of the heat of each part with time during the charging process. Obviously, the change of the heat stored in the HSB increases linearly during the charging process. For the charging condition in the large temperature difference mode, the heat growth curve is steeper, indicating that the accumulated heat in the HSB grows faster. In addition, the size of the same type of heat at the end of heat charging is basically the same under different heat charging modes. When the average temperature

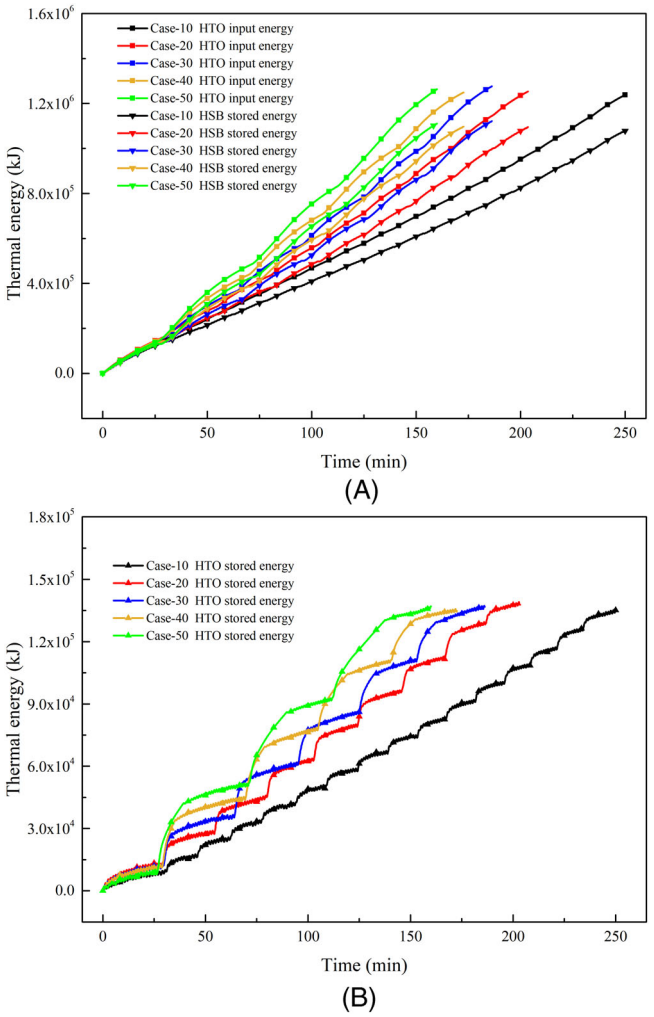

FIGURE 10 HTO input energy and HSB stored energy change during the charging process A, and HTO stored energy changes during the charging process B

of the HSB reaches 260°C, the charging is completed. The amount of heat entering the thermal storage unit under different charging modes is 1.24×10^6-1.28×10^6 kJ, and the average heat input is about 1.26×10^6 kJ; the heat stored in HSB is 1.08×10^6-1.11×10^6 kJ, and the average heat storage is about 1.10×10^6 kJ; and the heat of the HTO inside the heat storage unit stored in the whole charging process is about 1.36×10^5 kJ, accounting for the total heat input to the heat storage unit of 10.8%. The heat stored by the solid HSB occupies a large proportion, but the heat stored by the HTO in the unit's internal cavity is still the device's practical heat storage and can be utilized.

4.5 | The heat-release power of oil during charging

To explore the rate at which heat is transported to the SHSU through the working fluid during the whole

charging process, we define the HTO's heat-release power by Equation (1). As shown in Figure 11A, the HTO heat-release power variation trend with time under different charging modes is roughly the same. In the early stage of charging, due to the immense heat transfer temperature difference between the working fluid and the HSB, the corresponding HTO heat-release power is also more significant. Then the heat-release power decreases as the temperature difference gradually becomes smaller. With the progress of the charging process, the HTO's heat-release power curve gradually develops horizontally, indicating that the power tends to a constant value. This phenomenon is more evident in the heat charging mode like Case-10. However, an enormous temperature difference in charging mode brings a higher heat transfer rate, thus showing a more considerable heat-release power. In the range of experimental conditions, when the charging temperature difference is slight, such as the charging mode in Case-10, the average heat-release power of HTO is only 82.6 kW, as shown in Figure 11B. While the charging is carried out in a mode with a significant temperature difference, such as Case-50, the HTO's heat-release power increases to 131.6 kW, increasing 59.3%. Obviously, increasing the heat transfer temperature difference in the heat charging process can significantly accelerate the transfer of heat from HTO to SHSB.

4.6 | The charging power of SHSB

Figure 12A shows the power change curve of the HSB during the heat storage process and the average heat storage power diagram of the heat charging process under different working conditions. During the whole charging experiment, the changing trend of the heat storage power of the HSB and the HTO's heat release power is the same.

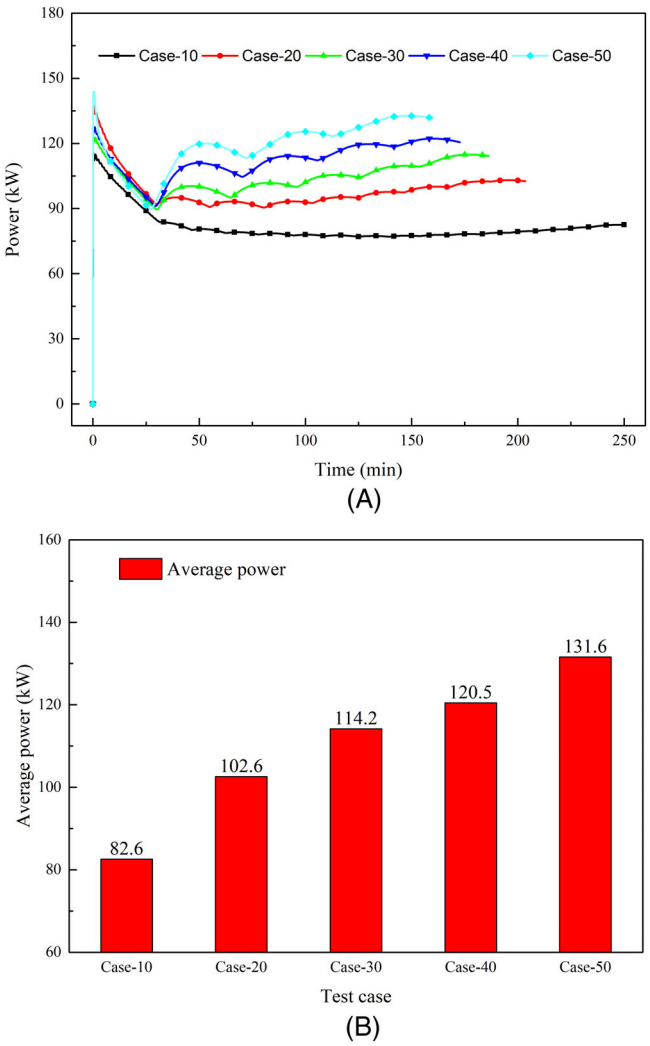

FIGURE 11 The power of HTO during the charge A, and the average power of the whole charging process B

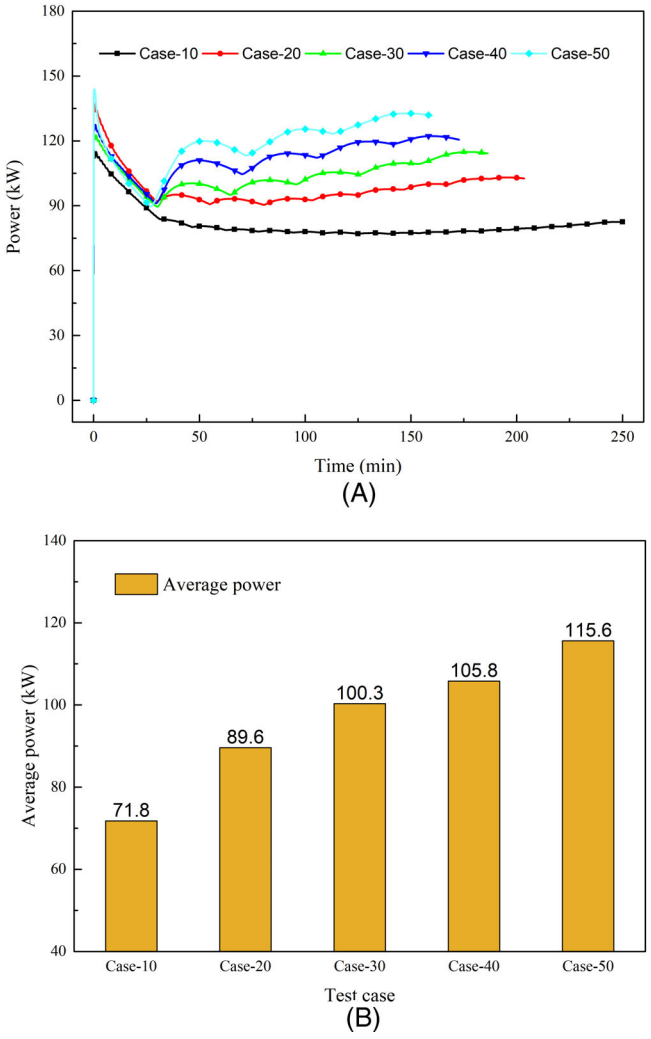

FIGURE 12 The power of the HSB during the charge A, and the average power of the whole charging process B

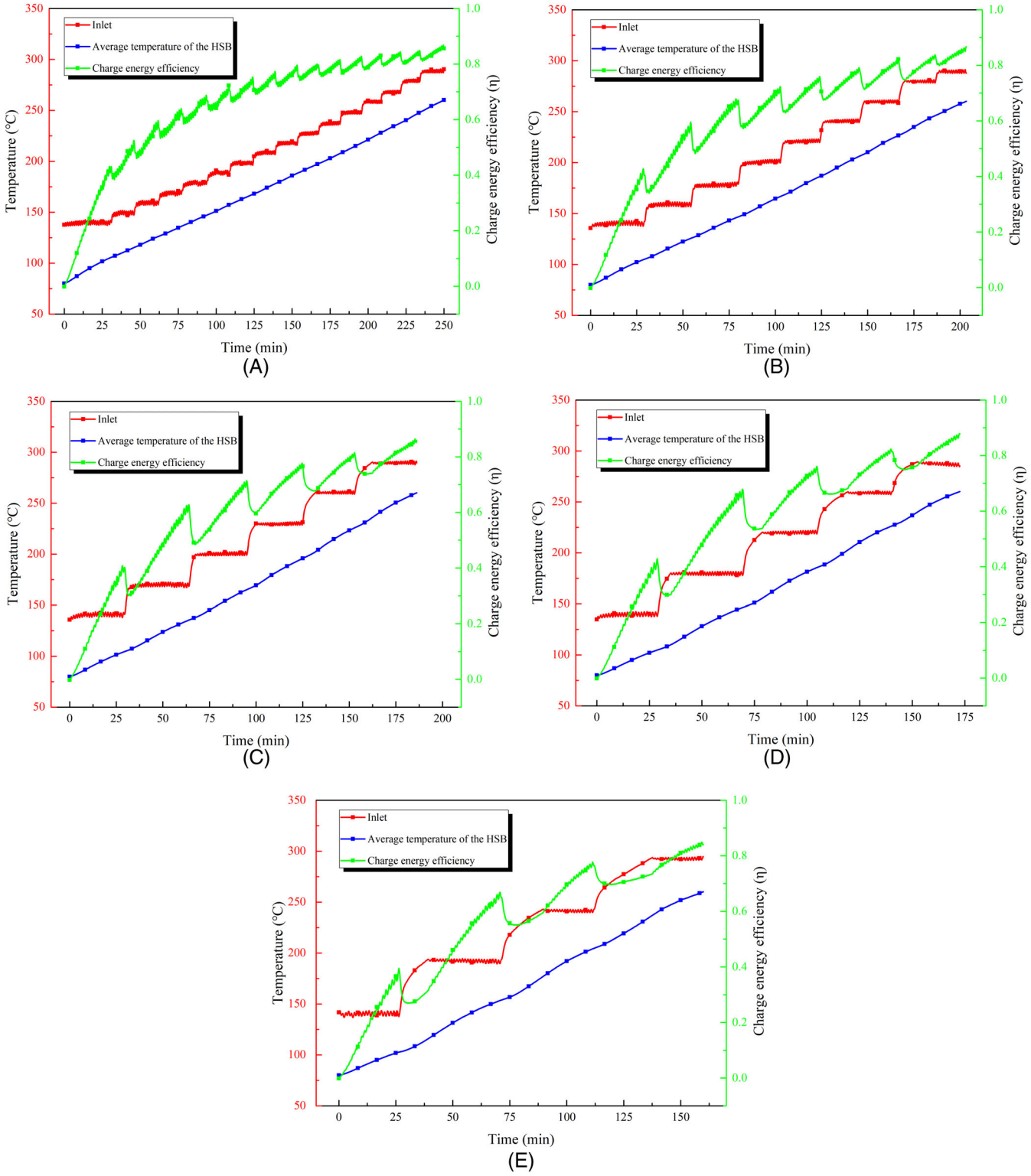

FIGURE 13 Charge energy efficiency and temperature evolution during charging

As the heat charging progresses, the heat storage power gradually tends to a particular value. Due to the heat transfer temperature variation, the charging power of SHSB fluctuates accordingly during the charge. In the thermal charging experiment with a slight temperature difference, the power is relatively stable during the thermal charging process, while the experimental conditions with a significant temperature difference are the opposite. In addition, the working conditions in the large temperature difference charging mode can obtain higher

charging power, and more thermal energy is accumulated inside the HSB simultaneously. For example, in Figure 12B, the Case-50 charging mode obtained 115.6 kW of charging power, while the Case-10 is only 71.8 kW. As shown in Figure 11B and Figure 12B, with the temperature difference between charging heat increases, the increment has a specific reduction in the average HTO's heat-release power and the average heat storage power of the HSB.

4.7 | Charge energy efficiency and normalized charge energy efficiency

Figure 13 shows the charge energy efficiency and temperature variation curves with time during the charging process under different experimental conditions. During the whole charging process, due to the variable temperature rise charging mode, the charging energy efficiency dynamically increases from 0 at the beginning of charging to about 0.83 at the end of charging; there are fluctuations in the charging process, and the amplitude and frequency of energy efficiency fluctuations vary by performing different charging modes.

To quantify the efficiency of the charging process and consider the influence of the charging time, we define the normalized charge energy efficiency to evaluate and analyze the efficiency of the charging process under different charging modes. The normalized charge energy efficiency is shown in Figure 14. The whole charging process shows better efficiency for the mode with a minor temperature difference. The normalized energy efficiency corresponding to Case-10 is 64.5%, while the normalized energy efficiency corresponds to Case-50 with a significant temperature difference is only 34.8%. Although the charging in the large temperature difference mode can bring a more significant charging rate, the HSB in the SHSU in this charging mode has low utilization efficiency of the heat entering the SHSU during the entire charging process.

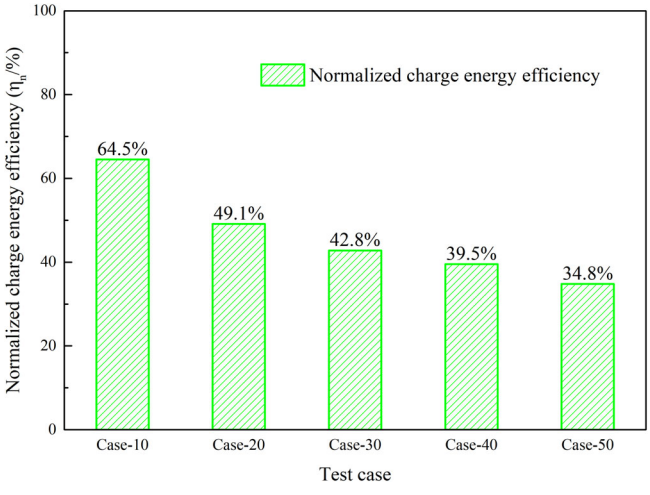

FIGURE 14 Normalized charge energy efficiency

4.8 | Uncertainty analysis

The temperature and flow rate uncertainties are 0.05% and 1% respectively. As shown in Table 3, the uncertainties are estimated for the energy, power, and other Parameters.

5 | CONCLUSION

In this article, a heat storage unit with the circular channel HSB immersed by HTF is charged under different temperature difference modes, and the temperature, thermal energy and power changes of the HTO working fluid and the HSB during the whole charging process are studied. A quantitative efficiency evaluation index on a time scale is defined to compare the relative value of the charge energy efficiency in the charging process of SHSU. The specific conclusions are as follows:

1. Since the heat transfer temperature difference during the charge is maintained in a specific range, the temperature change trend of the HSB under different temperature difference modes increases linearly, and the temperature and time of the HSB in the charging mode with a slight temperature difference have a better linear relationship.

TABLE 3 The uncertainty of experimental results

Parameters	Meaning	Uncertainty
$\rho(T)$	The density of the heat transfer oil	± 4.07%
$c_p(T)$	The specific heat of the heat transfer oil	± 0.02%
E	The cumulative energy	± 4.19%
P	The average power	± 4.19%
Q_{oil}	The heat stored in the oil	± 4.07%
Q_{lose}	The heat lose	± 1%
$Q_{cha.storage}$	The storage heat during charging	± 5.84%
η_e	The charge energy efficiency	± 0.13%
η_n	The normalized charge energy efficiency	± 2.36%

2. Increasing the heat transfer temperature difference in the charging process can significantly shorten the charging time and quickly complete the charging of the SHSU. In the experimental conditions, the time of the charging mode with a significant temperature difference is shortened by 36.1% compared with the charging mode with a slight temperature difference.
3. When the HSB reaches the predetermined 260°C, the charging mode with different temperature differences will not significantly affect the temperature of the HTO at the unit's outlet. The outlet temperature under different working conditions is about 272°C.
4. Whether it is the thermal energy release power of the HTO or the thermal energy storage power of the HSB, the power can be improved in the charging mode with a significant temperature difference. The maximum increase in the charging experiment is 59.3% and 61.0% respectively. The corresponding power is 131.6 and 115.6 kW respectively.
5. The charging energy efficiency of the SHSU fluctuates from 0 to 0.83 during the entire charging process. While increasing the heat transfer temperature difference during the charging reduces the normalized energy efficiency; the value is reduced from 64.5% for Case-10 to 34.8% for Case-50; that is, the heat transfer method with a significant temperature difference does not mean that the energy can be fully utilized effectively.

This research can be influential in heat storage design and industrial applications. To more comprehensively evaluate the performance of this type of heat storage, we should also research the heat release performance under different temperature difference modes in the future to provide data and experience support for the design and operation of the thermal energy storage device.

NOMENCLATURE

c_p	the specific heat capacity of HTO (kJ/kg K)
$c_p(T)$	the specific heat capacity function of HTO (kJ/kg K)
E	the total energy released or absorbed by the HTF in the SHSU (kJ)
P	the average power (kW)
$\rho(T)$	the density function of HTO (kg/m^3)
$Q_{\text{cha.storage}}$	the energy stored by HSB during charging (kJ)
$Q_{\text{cha.oil}}$	the energy stored by the HTO during charging (kJ)
$Q_{\text{cha.lose}}$	the heat loss during charging (kJ)
Q_{oil}	the energy stored in the HTO (kJ)
q_m	the mass flow rate (kg/s)
q_v	the volume flow (m^3/s)
T	the temperature (K)
t	the charging experiment (minute)
t_{max}	maximum time of all experiments (minute)
t_x	the time spent in a particular charge (minute)

Acronyms

HSB	heat storage body
HTF	heat transfer fluid
HTO	heat transfer oil
SHSU	sensible heat storage unit

Subscripts

ave	the average
cha	the charging process
i	initial
in	the inlet
out	the outlet

Greek symbols

ρ	the density of HTO (kg/m^3)
η_e	the charge energy efficiency
η_n	the normalized charge energy efficiency

ACKNOWLEDGEMENTS

This work was supported by the National Natural Science Foundation of China (52036008).

CONFLICT OF INTEREST

The authors declare that they have no known competing financial interests or personal relationships that could have appeared to influence the work reported in this paper.

REFERENCES

1. Gautam A, Saini RP. A review on technical, applications and economic aspect of packed bed solar thermal energy storage system. *J Energy Storage*. 2020;27:101046. doi:10.1016/j.est.2019.101046
2. Dong H, Liu Y, Zhao Z, Tan X, Managi S. Carbon neutrality commitment for China: from vision to action. *Sustain Sci*. 2022;17:1741-1755. doi:10.1007/s11625-022-01094-2
3. Wan B, Tian L, Fu M, Zhang G. Green development growth momentum under carbon neutrality scenario. *J Clean Prod*. 2021;316:128327. doi:10.1016/j.jclepro.2021.128327
4. Uz D, Chim C. Intermittency in wind energy and emissions from the electricity sector: evidence from 13 years of data. *Sustain*. 2022;14:23-29. doi:10.3390/su14042242
5. Zhou S, Wang Y, Zhou Y, Clarke LE, Edmonds JA. Roles of wind and solar energy in China's power sector: implications of intermittency constraints. *Appl Energy*. 2018;213:22-30. doi:10.1016/j.apenergy.2018.01.025
6. Yang T, Liu W, Kramer GJ, Sun Q. Seasonal thermal energy storage: a techno-economic literature review. *Renew Sustain Energy Rev*. 2021;139:110732. doi:10.1016/j.rser.2021.110732

7. Feng PH, Zhao BC, Wang RZ. Thermophysical heat storage for cooling, heating, and power generation: a review. *Appl Therm Eng*. 2020;166:114728. doi:10.1016/j.applthermaleng.2019.114728
8. Waked AM. Solar energy storage in rocks. *Sol Wind Technol*. 1986;3:27-31. doi:10.1016/0741-983X(86)90045-7
9. Marti L, Puertas R. Sustainable energy development analysis: energy trilemma. *Sustain Technol Entrep*. 2022;1:100007. doi:10.1016/j.stae.2022.100007
10. Sorour MM. Performance of a small sensible heat energy storage unit. *Energy Convers Manage*. 1988;28:211-217. doi:10.1016/0196-8904(88)90024-6
11. Keilany MA, Milhé M, Bézian JJ, Falcoz Q, Flamant G. Experimental evaluation of vitrified waste as solid fillers used in thermocline thermal energy storage with parametric analysis. *J Energy Storage*. 2020;29:101285. doi:10.1016/j.est.2020.101285
12. Dutta R, Sandilya P. Experimental investigations on cold recovery efficiency of packed-bed in cryogenic energy storage system. *IOP Conf Ser Mater Sci Eng*. 2020;755:012103. doi:10.1088/1757-899X/755/1/012103
13. Soprani S, Marongiu F, Christensen L, et al. Design and testing of a horizontal rock bed for high temperature thermal energy storage. *Appl Energy*. 2019;251:113345. doi:10.1016/j.apenergy.2019.113345
14. Salomoni VA, Majorana CE, Giannuzzi GM, et al. Thermal storage of sensible heat using concrete modules in solar power plants. *Sol Energy*. 2014;103:303-315. doi:10.1016/j.solener.2014.02.022
15. Vigneshwaran K, Singh Sodhi G, Muthukumar P, Subbiah S. Concrete based high temperature thermal energy storage system: experimental and numerical studies. *Energy Convers Manage*. 2019;198:111905. doi:10.1016/j.enconman.2019.111905
16. Kumar R, Patil AK, Kumar M. Charging and discharging characteristics of sensible energy storage system with multiple cylindrical passages. *J Energy Resour Technol Trans ASME*. 2021;143:2-7. doi:10.1115/1.4051395
17. Kumar R, Pathak AK, Kumar M, Patil AK. Experimental study of multi tubular sensible heat storage system fitted with wire coil inserts. *Renew Energy*. 2021;164:1244-1253. doi:10.1016/j.renene.2020.10.058
18. Kumar R, Kumar M, Patil AK. Capacity factor characteristics for a multi-tubular sensible energy storage system with wire coil inserts. *Int J Energy Res*. 2022;46:4540-4549. doi:10.1002/er.7447
19. Bindra H, Bueno P, Morris JF, Shinnar R. Thermal analysis and exergy evaluation of packed bed thermal storage systems. *Appl Therm Eng*. 2013;52:255-263. doi:10.1016/j.applthermaleng.2012.12.007
20. Al-Azawii MMS, Theade C, Danczyk M, Johnson E, Anderson R. Experimental study on the cyclic behavior of thermal energy storage in an air-alumina packed bed. *J Energy Storage*. 2018;18:239-249. doi:10.1016/j.est.2018.05.008
21. Öztürk HH. Comparison of energy and exergy efficiencies of an underground solar thermal storage system. *Int J Energy Res*. 2004;28:341-353. doi:10.1002/er.968
22. Skinner JE, Strasser MN, Brown BM, Selvam RP. Testing of high-performance concrete as a thermal energy storage medium at high temperatures. *J Sol Energy Eng Trans ASME*. 2014;136:1-6. doi:10.1115/1.4024925
23. Gunes S, Ozceyhan V, Buyukalaca O. Heat transfer enhancement in a tube with equilateral triangle cross sectioned coiled wire inserts. *Exp Therm Fluid Sci*. 2010;34:684-691. doi:10.1016/j.expthermflusci.2009.12.010
24. Moffat RJ. Contributions to the theory of single-sample uncertainty analysis. *J Fluids Eng Trans ASME*. 1982;104:250-258. doi:10.1115/1.3241818

How to cite this article: Cheng F, Zou Y, Huang S, et al. Testing of the oil-immersed sensible heat storage unit with circular channel solid heat body under charging modes with different heat transfer temperature difference. *Int J Energy Res*. 2022;46(15):24487-24500. doi:10.1002/er.8765